

CORRECTION

Adaptation is not required to explain the long-term response of axons to molecular gradients

Jun Xu¹, William J. Rosoff¹, Jeffrey S. Urbach² and Geoffrey J. Goodhill^{3,*}

¹Department of Neuroscience, Georgetown University Medical Center, 3900 Reservoir Road NW, Washington, DC 20007, USA

²Department of Physics, Georgetown University, 37th and O Streets NW, Washington, DC 20057, USA

³Queensland Brain Institute, Department of Mathematics and Institute for Molecular Bioscience, University of Queensland, St Lucia, QLD 4072, Australia

There was an error published in *Development* **132**, 4545–4552.

The sentence on page 4550 ‘Following Berg and Purcell (Berg and Purcell, 1977), threshold detection of the gradient occurs when:

$$\bar{b}_i(t) = \sum_j \bar{b}(t) e^{-(\phi_i - \phi_j)^2 / 2\sigma_s^2},$$

where δ_{bin} is the uncertainty in the concentration measurement for one bin.’

should instead have read:

‘Following Berg and Purcell (Berg and Purcell, 1977), threshold detection of the gradient occurs when:

$$(n - k)m = \frac{\sqrt{2}\delta_{\text{bin}}}{\sqrt{k}},$$

where δ_{bin} is the uncertainty in the concentration measurement for one bin.’

The publishers apologise to the authors and readers for this mistake.

Adaptation is not required to explain the long-term response of axons to molecular gradients

Jun Xu¹, William J. Rosoff¹, Jeffrey S. Urbach² and Geoffrey J. Goodhill^{3,*}

¹Department of Neuroscience, Georgetown University Medical Center, 3900 Reservoir Road NW, Washington, DC 20007, USA

²Department of Physics, Georgetown University, 37th and O Streets NW, Washington, DC 20057, USA

³Queensland Brain Institute, Department of Mathematics and Institute for Molecular Bioscience, University of Queensland, St Lucia, QLD 4072, Australia

*Author for correspondence (e-mail: g.goodhill@uq.edu.au)

Accepted 5 August 2005

Development 132, 4545-4552

Published by The Company of Biologists 2005

doi:10.1242/dev.02029

Summary

It has been suggested that growth cones navigating through the developing nervous system might display adaptation, so that their response to gradient signals is conserved over wide variations in ligand concentration. Recently however, a new chemotaxis assay that allows the effect of gradient parameters on axonal trajectories to be finely varied has revealed a decline in gradient sensitivity on either side of an optimal concentration. We show that this behavior can be quantitatively reproduced with a computational model of axonal chemotaxis that does not employ explicit adaptation. Two crucial components of this model required to reproduce the observed sensitivity are spatial and

temporal averaging. These can be interpreted as corresponding, respectively, to the spatial spread of signaling effects downstream from receptor binding, and to the finite time over which these signaling effects decay. For spatial averaging, the model predicts that an effective range of roughly one-third of the extent of the growth cone is optimal for detecting small gradient signals. For temporal decay, a timescale of about 3 minutes is required for the model to reproduce the experimentally observed sensitivity.

Key words: Axon guidance, Chemotaxis, Computational model, Nerve growth factor, Dorsal root ganglion

Introduction

Axons use many types of navigational cues to find appropriate targets in the developing nervous system (Dickson, 2002; Huber et al., 2003; Guan and Rao, 2003). A particularly important class of guidance signal directing axonal growth is molecular gradients (e.g. Tessier-Lavigne and Placzek, 1991; Baier and Bonhoeffer, 1992; Tessier-Lavigne and Goodman, 1996; Song and Poo, 1999). The response to such gradients is primarily mediated by the growth cone, the motile structure at the tip of developing axons (Gordon-Weeks, 2000). The growth cone turns in response to an external ligand gradient, presumably as a result of asymmetric intracellular signaling that arises from the difference in receptor occupancy across its spatial extent. Some progress has recently been made in uncovering the molecules involved in the signal transduction networks underlying gradient detection in growth cones (Song and Poo, 2001; Guan and Rao, 2003). However, the overall gradient detection algorithm these transduction networks implement is unknown.

A key aspect of the chemotropic response of many types of cells is adaptation, which has been defined as the continual adjustment of the baseline against which further increases in concentration are compared (Bray, 2001). This has been particularly well studied in the context of bacteria (e.g. Macnab and Koshland, 1972; Koshland et al., 1982; Barkai and Leibler, 1997). It is thus a reasonable hypothesis that growth cones might also implement adaptation to gradients, which would

mean that they display a similar sensitivity to small concentration differences of an external ligand over a wide range of background concentrations of the ligand. This would allow growth cones to be guided over a greater distance by a single gradient (Goodhill, 1998; Goodhill and Urbach, 1999) than growth cones that do not adapt. Perhaps the most explicit proposal of this hypothesis has been made by Ming et al. (Ming et al., 2002). Using gradients established by a pipette, they tested the change in responsiveness of *Xenopus* spinal growth cones to a steep gradient when a sudden change in background concentration was introduced. In each case, the concentration of ligand at the growth cone was about 0.1 nM, the change in concentration across 10 microns was about 10% (Zheng et al., 1994), and the sudden changes in background concentration were about 0.1 nM (for ease of comparison we have converted the ng/ml units originally quoted to molar units). There was thus at most an approximate twofold increase in the absolute concentration of ligand at the growth cone. Under these conditions a rapid initial desensitization was observed whereby the growth cone could no longer respond to the 10% gradient, which was followed by a more prolonged period of resensitization (Ming et al., 2002). The timescale of desensitization and resensitization has recently been investigated in more detail by Piper et al. (Piper et al., 2005).

However, the experiments of Ming et al. (Ming et al., 2002) examined only the relatively short-term temporal dynamics of the response of growth cones to small step changes in

concentration. They did not explicitly test the hypothesis that growth cones display a similar sensitivity to small concentration differences across a wide range of background concentrations. A recent experiment has addressed this more directly by examining the long-term response of axons in a three-dimensional collagen gel environment to gradients of precisely controlled steepness and shape (Rosoff et al., 2004). Explants of rat dorsal root ganglia (DRGs) were grown for 2 days in gradients of nerve growth factor (NGF) of a steepness of 0.2% per 10 microns at background concentrations varying from 0.0001 nM to 100 nM, and the degree of asymmetry in the outgrowth was quantified. A simple interpretation of the adaptation hypothesis would predict that the guidance response should be roughly constant over this range, as the stimulus (fractional change in concentration across the growth cone) is the same in each case. However, this is not what was observed: instead the guidance response peaked in the range 1-10 nM, and declined at both higher and lower concentrations, falling to zero at the two ends of the concentration scale.

We decided to rigorously test whether this result is indeed consistent with a non-adapting gradient detection mechanism by constructing a computational model of growth-cone sensing and movement. Using the data of Rosoff et al. (Rosoff et al., 2004) to constrain the parameters of the model, we show that it is possible to produce a close quantitative match between model and data without invoking explicit adaptational mechanisms. In addition, we find that both spatial and temporal averaging of the stochastic receptor-binding signal are required to produce the exquisite level of sensitivity observed experimentally. Spatial and temporal averaging can be interpreted as corresponding, respectively, to the spatial spread of signaling effects downstream from receptor binding, and to the finite time over which these signaling effects decay. For spatial averaging the model predicts that an effective range of roughly one-third of the extent of the growth cone is optimal, whereas for temporal averaging a timescale of about 3 minutes is required for the model to reproduce the experimentally observed sensitivity.

Materials and methods

Mathematical model

The model consists of a two-dimensional, semi-circular growth cone, the one-dimensional edge of which is covered in receptors for the diffusible ligand. The receptors are redistributed according to a uniform random distribution at every time step. Here, we present a more intuitive description of the model; a more mathematical description is given below under the heading 'Equations of the model'.

Model description

At each time step in the model, the probability p_i for receptor i to be bound is given by $p_i = C_i / (C_i + K_D)$, where C_i is the external ligand concentration at the position of receptor i and K_D is the dissociation constant for the receptor-ligand complex. This gives a highly noisy measurement of differences in concentration around the growth cone that arise from the presence of an external gradient. The experimental data of Rosoff et al. (Rosoff et al., 2004) suggests that growth cones must be averaging concentration measurements to achieve their exquisite sensitivity to gradients, as the noise present in an instantaneous measurement of the local concentration is much larger than the gradient signal itself. In the model, we include both spatial and temporal averaging before each movement event is

initiated (see below). In temporal averaging, the recent history of the binding state of the receptor is pooled according to a decaying function of time, which we assume to be a half-gaussian of variance σ_t . For small σ_t , only the immediate binding state of each receptor is considered; for large σ_t , a long history of binding is averaged. σ_t trades off noise in concentration measurements against temporal locality: a large σ_t increases the accuracy of the concentration measurement but decreases its temporal resolution so that it cannot respond to rapidly changing signals, whether due to changes in the concentration field itself or to movement of the growth cone within a fixed concentration field. In spatial averaging, the binding of a spatially distributed set of receptors is pooled to determine a binding density at each point. This is achieved in the model by convolving the receptor-binding density (from either a single or temporally averaged measurement) with a gaussian function of variance σ_s . For small σ_s , just a few neighboring receptors are averaged; for large σ_s , a significant proportion of all of the receptors on the growth cone are included in the average. σ_s trades off noise in concentration measurements against spatial locality: a large σ_s increases the accuracy of the concentration measurement, but decreases the spatial precision in a concentration measurement, which is key to measuring a gradient. For very large σ_s , all spatial locality is lost, and the binding at each point equals the average concentration across the entire growth cone.

Once a receptor-binding density as a function of angle around the growth cone has been calculated, the growth cone picks the direction in which this is maximum. We do not model how this occurs, but there are several possibilities for performing this type of amplification (e.g. Parent and Devreotes, 1999; Meinhardt, 1999; Iglesias and Levchenko, 2002) (see also Discussion). Because axons tend to grow in straight lines (Bray, 1979; Katz, 1985), we allowed the axon to change direction only slightly in response to this gradient signal: the new angle of growth is $(1-\alpha)$ times the old direction plus α times the new direction, where α is close to zero. The growth cone then takes a small, constant, step forward. We refer to α as 'momentum'. Note that there is no explicit adaptation to external ligand levels in this model, as in for instance Barkai and Leibler (Barkai and Leibler, 1997).

Equations of the model

The concentration of ligand $C(\vec{r})$ at position $\vec{r} = x\hat{i} + y\hat{j}$ in the gradient, where \hat{i} and \hat{j} are unit vectors perpendicular and parallel, respectively, to the direction of the gradient, is given by:

$$C(\vec{r}) = C_0 e^{gy},$$

where g is the gradient steepness and C_0 is a reference concentration. The binding $b_i(t)$ of receptor i at position \vec{r}_i at time t is then set to 1 with probability p_i and 0 with probability $(1-p_i)$, where:

$$p_i = \frac{C(\vec{r}_i)}{C(\vec{r}_i) + K_D}.$$

The temporally averaged binding at each binding site, \bar{b}_i , is given by:

$$\bar{b}_i(t) = \sum_{\tau=0}^t b_i(\tau) e^{-(t-\tau)^2/2\sigma_t^2}.$$

The spatially averaged binding at each site, $\bar{\bar{b}}_i(t)$, is given by:

$$\bar{\bar{b}}_i(t) = \sum_j \bar{b}_j(t) e^{-(\phi_i - \phi_j)^2/2\sigma_s^2}.$$

where ϕ_i is the angular position on the growth cone of receptor i . We do not explicitly normalize the results of spatial and temporal averaging, as we are only interested in the position of maximum binding. The angle of maximum binding ϕ_{max} is set to the angle ϕ_i of

the receptor with maximum \bar{b}_i . The overall direction $\theta(t)$ of the growth cone is updated according to

$$\theta(t) = (1-\alpha)\theta(t-1) + \alpha\hat{\phi}_{max}(t).$$

The growth cone then takes a small step forwards in this new direction. The only random component in the model is the receptor binding at each step, which is intrinsically stochastic, and no additional noise is added to this.

Comparison with experimental data

Examples of the explant data generated by Rosoff et al. (Rosoff et al., 2004) are shown in Fig. 1A,B. Rosoff et al. (Rosoff et al., 2004) quantified the response of axons to gradients by the ‘guidance ratio’: the number of pixels representing neurites on the up-gradient side of the explant U was compared with that on the down-gradient side D , with the guidance ratio defined as $(U-D)/(U+D)$. This was calculated for digital images of the explants at 640 by 480 resolution.

In order to match our computational simulations to these experimental results, we generated digital images of simulated explants at the same resolution. Simulation parameters were chosen to match the mean experimental values for average neurite number and length, explant radius (all simulated explants were circles), and growth cone diameter. The starting point for each axonal trajectory was a random position within the explant, and the initial direction was random. To represent the likelihood that not all neurites in the experimental condition are actually responsive to NGF, i.e. that some neurites do not express TrkA (Gallo et al., 1997), we assumed that only a proportion of simulated neurites per explant were actually responsive to the gradient. Non-responsive growth cones in the simulations grew simply according to random fluctuations in receptor binding with no gradient. Simulated explants were grown in identical gradients to those used experimentally, i.e. exponential with a fractional change 0.1, 0.2 or 0.4% over 10 microns, at an absolute

concentration ranging from 0.0001 nM to 100 nM. Images of neurite trajectories were generated using the Matlab ‘plot’ command with the ‘linewidth’ parameter chosen to match the width of neurites observed experimentally. The guidance ratio was then calculated as for the experimental explants. We also investigated a more controlled method of generating pixels to represent the trajectories, based on an optics-based model for how images were generated experimentally by Rosoff et al. (Rosoff et al., 2004). However, this produced guidance ratios that were not significantly different from those produced by the ‘plot’ method.

Parameter values

Parameter values used are shown in Table 1. The upper block of values were determined directly from experimental measurements (Rosoff et al., 2004). Note that in the model there is no ‘absolute concentration’ of ligand, rather all concentrations are expressed relative to K_D . The proportion of responsive neurites is consistent with experimental estimates of the proportion of TrkA-positive neurons in early postnatal rat DRGs (Mu et al., 1993; Phillips and Armanini, 1996; Bennett et al., 1996; Molliver and Snider, 1997). The number of receptors is in the middle of the range of estimates of the number of neurotrophin receptors on embryonic sensory neurons (Meakin and Shooter, 1992).

The timestep δ_t is the basic unit of time in the model: the time over which a concentration measurement is made and over which a small movement occurs. We assume that, at successive timesteps, the growth cone makes a statistically independent measurement of the binding of each receptor. This provides a lower bound on the size of the timestep; for diffusion-limited receptor-binding kinetics the minimum time between statistically independent binding events can be estimated as the radius of the sensing device squared, divided by the diffusion constant (Berg and Purcell, 1977). For diffusion constants in the range 10^{-6} to 10^{-7} cm²/second, this time is between 1 and 10 seconds [Rosoff et al. (Rosoff et al., 2004) measured a value of 8×10^{-7} cm²/second for the diffusion of NGF in collagen]. An upper bound is provided by the fact that measurable changes in growth cone morphology in response to external cues can be seen on a timescale of 1 minute or less (e.g. Zheng et al., 1996); 30 seconds was chosen as an intermediate between these limits.

An appropriate value for the momentum α is constrained by the maximum rate at which growth cones can turn. In the model, this is set by the timestep δ_t , as well as by α . A strong gradient (sufficient to dominate binding noise) perpendicular to the direction of travel of the axon will produce a signal at $\pi/2$. In a single timestep, the change in the angle of the axon will be $\alpha\pi/2$. The growth cone will turn 45 degrees towards the direction of the gradient after approximately $(\pi/4)/\alpha\pi/2=1/(2\alpha)$ steps. Thus, the fastest observable turning time,

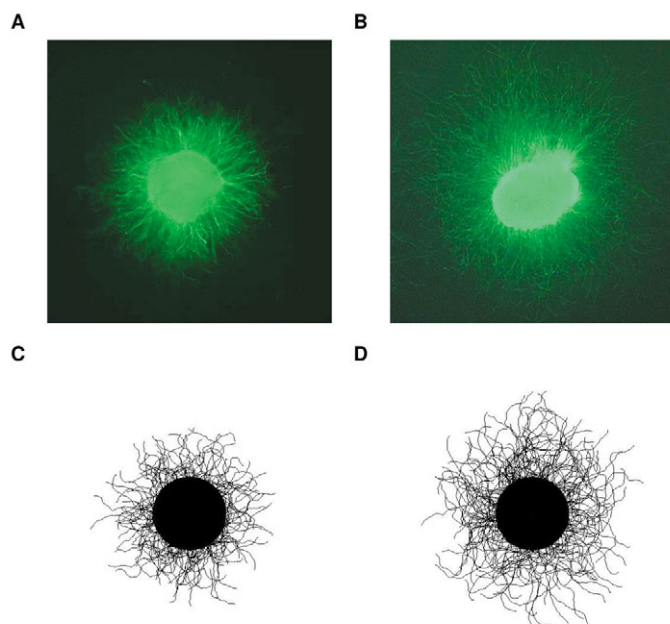


Fig. 1. Typical dorsal root ganglia (DRG) explants generated experimentally by Rosoff et al. (Rosoff et al., 2004) (A,B), and by the computational model (C,D). In A,C, there is no nerve growth factor (NGF) gradient; in B,D, an exponential NGF gradient is present increasing upwards in the figure with a fractional change of 0.2% over 10 μm . All images are 480×480 pixels and presented at the same scale. The diameter of the explants in the simulated cases is 700 μm .

Table 1. Parameters used in the model

| Parameter | Value* |
|---|---------------------------------------|
| Exponential gradient steepness | 0/0.1%/0.2%/0.4% per 10 μm |
| Ligand concentration at explants | 0.001-100 $\times K_D$ |
| Total outgrowth time | 40 hours |
| Explant radius | 350 μm |
| Number of neurites per explant | 200 |
| Length per neurite | 1100 μm |
| Growth cone diameter | 10 μm |
| Explants averaged per condition | 20 |
| Number of receptors on growth cone | 3000 |
| Proportion of responsive neurites | 60% |
| Timestep | 30 seconds |
| Momentum, α | 0.03 |
| Scale of temporal averaging, σ_t | 2 timesteps (60 seconds) |
| Scale of spatial averaging, σ_s | 5% of growth cone circumference |

*Values in the upper block were taken directly from the experimental results of Rosoff et al. (Rosoff et al., 2004). For further explanation see Materials and methods.

T_{min} , is equal to $\delta_t/(2\alpha)$ seconds. Changes in the timestep must therefore be accompanied by proportional changes in α to keep a constant response time. Experimentally T_{min} is in the order of 10 minutes, so $\alpha=30/1200\approx 0.03$ for $\delta_t=30$ seconds.

The momentum is also constrained by the degree to which axonal trajectories meander. In the absence of a gradient, the growth cone executes a random walk in angle space. Each timestep, the orientation of the growth cone changes by some amount δ_θ uniformly distributed in $[-\alpha\pi/2, \alpha\pi/2]$. Consider first the case with no temporal averaging. By the central limit theorem, after N statistically independent steps a collection of axons will display a distribution of changes in orientation with a spread given by $\Delta\theta_{rms}\sim\sqrt{N}\langle|\delta_\theta|\rangle=\sqrt{N}\alpha\pi/2\sqrt{3}$. Experimentally, even after 36 hours (approximately 2000 minutes), most of the axons have not changed direction by more than $\pi/2$. Thus, $\sqrt{2000}\cdot 60/\delta_t\alpha\pi/4<\pi/2$, or $\alpha<2\sqrt{\delta_t}/1.2\times 10^5=0.03$. To keep the trajectory meandering constant, α must change proportional to the square root of the timestep. When temporal averaging is used, the chosen orientation in successive timesteps is not statistically independent. The longer the temporal averaging time, the more likely it is that the position of maximum binding stays in approximately the same position. Roughly, the number of statistically independent steps is reduced from N to N/σ_t , and the average step size is increased from $\alpha\pi/4$ to $\sigma_t\alpha\pi/4$. From the arguments above, $\Delta\theta_{rms}\sim\sqrt{N/\sigma_t}\sigma_t\alpha\pi/4$. Thus, the meandering increases with the square root of the temporal averaging time.

For spatial averaging, we found there was a specific width σ_s that maximized the sensitivity of the growth cone (see Results), and it was this optimal value that we used in subsequent simulations. The duration of temporal averaging, σ_t , was determined as described in the Results. Simulations were coded in Matlab, and each explant took approximately 10 hours to run on a 3GHz Pentium 4 PC running Linux. The simulations shown here thus represent a total of approximately 2 years of CPU time.

Results

The computational model we consider is very simple: binding of ligand to receptors on the growth cone is averaged both temporally and spatially, and the growth cone then makes a small turn in the direction of maximum averaged binding (see Materials and methods). Typical results for the model using the parameters in Table 1 are shown in Fig. 1C,D, which can be compared with the experimentally generated explants.

Before matching the model to biological data it is important to understand the individual effect of some of the key parameters in the model. Fig. 2 shows how growth cone sensitivity, as measured by the guidance ratio (see Materials and methods), varies with the proportion of non-responsive neurites (Fig. 2A), the width of spatial averaging (Fig. 2B), and the duration of temporal averaging (Fig. 2C). In Fig. 2B, the width of spatial averaging, σ_s , is expressed as a percentage of the circumference of the semicircular growth cone. As σ_s increases the average is taken over more receptors and thus the noise in the local concentration measurements is reduced. Conversely, increasing σ_s implies less specificity in exactly where the concentration is measured, making the detection of a gradient more difficult. It can be seen that these two effects trade off to produce a peak in sensitivity at about $\sigma_s=5\%$. Because the total effective width of averaging is roughly $6\sigma_s$ ($3\sigma_s$ either side of the central point), this corresponds to a total width of about one-third of the distance around the growth cone. As was expected, in Fig. 2C, the longer the temporal averaging (the higher σ_t) the greater the sensitivity. We found

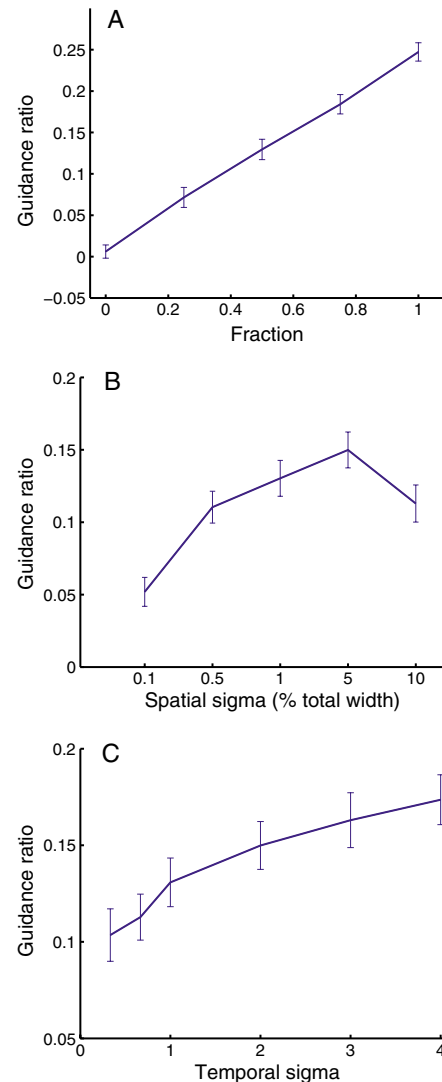


Fig. 2. Sensitivity of the model (as measured by the guidance ratio) to its parameters. (A) Proportion of neurites competent to respond to the gradient. Response increases roughly linearly with this proportion. (B) Width of spatial averaging, i.e. effective spatial spread of signaling effects downstream from receptor binding. Note the peak at 5%. (C) Duration of temporal averaging, i.e. the time over which signaling effects decay.

that a value of $\sigma_t=2$ was required to match the sensitivity of real axons (see below). This corresponds to looking back in time a total of about $3\sigma_t=6$ timesteps or 3 minutes. Beyond this the axon trajectories become more convoluted than those seen experimentally (data not shown), because a chance bias in binding on one side of the growth cone persists for many minutes.

We next proceeded to match the data in figure 3A,C of Rosoff et al. (Rosoff et al., 2004), by measuring how the response in the model varies as a function of gradient steepness (Fig. 3A) and absolute concentration (Fig. 3B). Explants were simulated in each case using the parameters in Table 1. (All simulated explants grew for 40 hours, whereas experimentally there was a range from 36–40 hours. We tested the effect of reducing the simulated time to 36 hours, and found no

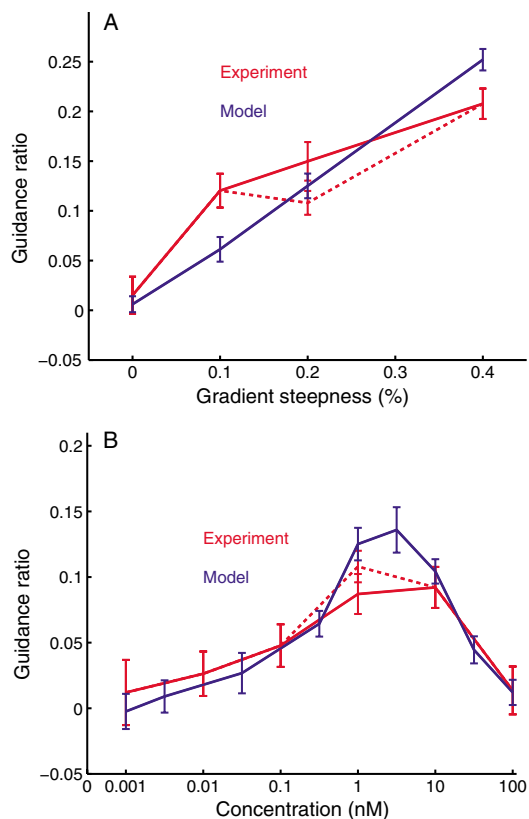


Fig. 3. Match of the model results to the experimental data of Rosoff et al. (Rosoff et al., 2004). Parameters used are shown in Table 1, with $K_D=3$ nM. (A) Response as a function of gradient steepness for an absolute concentration of 1 nM. (B) Response as a function of absolute concentration for a gradient steepness of 0.2%. The solid red curves show the data originally plotted by Rosoff et al. (Rosoff et al., 2004), whereas the dashed red curves show the revised experimental data that is obtained if all of the explants from the 0.2% gradient/1 nM condition are averaged together (see text).

significant change in the guidance ratio.) In terms of the absolute value of the guidance ratio, there is a fairly good match for each steepness of gradient. In the model, response varies close to linearly with gradient steepness, and this remains robustly true as the basic parameters are varied: these simply change the slope of the line (data not shown). The model curve shown therefore represents roughly the best linear approximation to the experimental data. Fig. 3B used exactly the same model parameters and shows a good match in the overall shape of the curve, particularly in the width of the peak, for guidance as a function of concentration for a fixed gradient steepness. [In the experimental data, the average guidance ratios for the 0.2% gradient/1 nM condition were slightly different between the steepness and concentration curves, as the two series of experiments were done at different times. Fig. 3A,B plot both the data as originally presented in Rosoff et al. (Rosoff et al., 2004), and the data obtained if all of the explants from the 0.2% gradient/1 nM condition in the two series of experiments are averaged together.] Note that perfect adaptation to the gradient signal would imply that this curve be flat, rather than peaked at an optimal concentration. The equations of the model are expressed relative to K_D , and thus

to plot model results on an absolute concentration scale requires a specific value for K_D to be chosen. This choice shifts the model curve in Fig. 3B to the left or the right, relative to the absolute concentration scale, without changing its shape. We found that assuming $K_D=3$ nM gave the best match with the experimental curve, which offered further support for the claim in Rosoff et al. (Rosoff et al., 2004) that the K_D underlying guidance in that system is in the range 1–10 nM. The fact that the falloff in sensitivity away from K_D is accurately described by the computational model is a strong indication that the limitation on gradient sensing in real growth cones is due to stochastic receptor binding.

The computational model allows two particular issues to be addressed regarding the experimental data. First, the guidance ratio does not take into account overlap pixels, i.e. pixels in the image where two neurites cross, which should in principle be counted twice. It is impossible to reliably identify these in the experimental data. However, in the simulations the actual trajectory of each neurite is precisely known, allowing overlap pixels to be double-counted if desired. We recalculated the guidance ratio with double counting, and found a small increase of about 20% that was consistent across gradient conditions (data not shown), owing to the fact that most double-pixels will be on the up-gradient side of the explant where there are more neurites. We thus conclude that, although this effect probably slightly reduces the guidance ratio values observed experimentally, it does not have an important impact on the overall shape of the response curves. None of the other results we report in this paper used double counting.

Secondly, the model can shed light on the relative importance of trophic versus tropic effects on explant asymmetry in NGF gradients. Could it be that the higher concentration of NGF on the up-gradient side of the explant simply promotes more growth on that side, causing a positive guidance ratio without actual guidance? Although this was discussed in Rosoff et al. (Rosoff et al., 2004), the model allows this question to be addressed more quantitatively. Explants were simulated with neurite growth cones that responded to the average concentration, as determined from the receptor binding, but were insensitive to variations in binding across their spatial extent. Neurite growth rate was now assumed to vary linearly with absolute concentration. We used the largest rate of change of outgrowth with concentration measured experimentally by Rosoff et al. (Rosoff et al., 2004), which occurred in the range 1 nM–3 nM. To maximize the possibility of seeing an effect, we simulated the steepest gradients investigated experimentally (0.4% per 10 μm), allowed 100% of simulated neurites to be responsive to the gradient, and took the absolute concentration to be K_D for maximum sensitivity. We found a guidance ratio of -0.00097 ± 0.0133 , showing that no significant guidance effect was induced by differential growth. The general point is that total outgrowth does not vary with concentration fast enough in the data of Rosoff et al. (Rosoff et al., 2004) to produce the observed asymmetry in the explants, given that the total change in concentration across an explant in these experiments is small.

In general, the response depends on both gradient steepness and absolute concentration. The experimental data of Rosoff et al. (Rosoff et al., 2004) presents only two one-dimensional cuts through a two-dimensional surface of growth cone response,

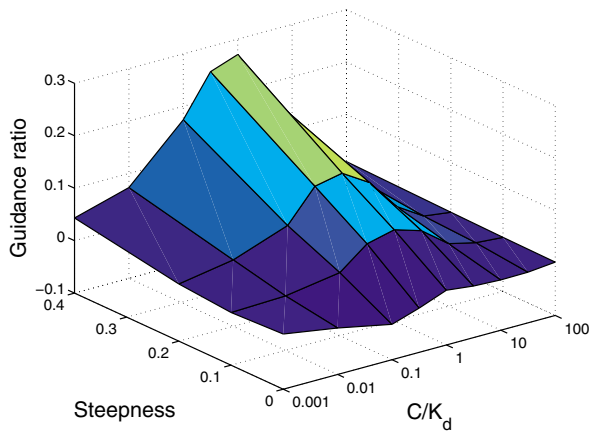


Fig. 4. The complete two-dimensional sensitivity surface for the model. Note that the peak along the concentration axis becomes higher and broader at the higher values of gradient steepness.

one along the steepness axis and one along the concentration axis. Having tuned the parameters of our model to match the data along these cuts as above, we then simulated the shape of the entire two-dimensional surface (Fig. 4). The most notable prediction is that the peak of response becomes broader as the gradient steepness is increased. When quantitative measurements of the actual concentration profiles of putative guidance molecules in vivo are available, the response surface represented in Fig. 4 can act as a guide to the feasibility of these gradients for actually guiding axons during development. This surface can also be used to predict the gradients required to promote the guided regrowth of axons in regeneration experiments.

Discussion

We have presented a computational model of gradient detection by growth cones that can reproduce the quantitative properties of the long-term response of real axons to gradients, as recently characterized by Rosoff et al. (Rosoff et al., 2004). The model shows that the bell-shaped response curve as a function of absolute concentration is consistent with the noise inevitably introduced by the stochastic nature of receptor binding. The gradient detection mechanism of the model does not include adaptation, at least at the level of the immediate effects of receptor binding, which is in contrast to models of bacterial chemotaxis, such as those of Barkai and Leibler (Barkai and Leibler, 1997) and Bray et al. (Bray et al., 1998).

It is clear from results using the pipette assay (e.g. Ming et al., 2002) that desensitization and resensitization of growth cones does occur. Although the results we have presented here and in Rosoff et al. (Rosoff et al., 2004) do not directly address these desensitization/resensitization processes, they provide evidence that such processes may not be implementing adaptation in the sense of a continual adjustment of the baseline against which further increases in concentration are compared (Bray, 2001). Desensitization/resensitization probably occur on a more rapid timescale than that over which growth cones experience significant concentration changes due to gradients in vivo (Piper et al., 2005), and growth cones

probably do not often experience sudden changes in concentration over their entire surface in vivo. Another study sometimes cited in support of growth cone adaptation is Rosentreter et al. (Rosentreter et al., 1998). This examined the response of retinal ganglion cells to gradients of tectal cell membrane density, and the authors argue that temporal retinal axons grew up a fixed increment of concentration, independent of both gradient steepness and starting concentration. The latter result suggests that retinal growth cones may 'adapt' in the sense of terminating their growth once they encounter a certain increase in ligand concentration relative to the concentration at which they first encountered the ligand. However, this is adaptation in a different sense to that discussed in this paper. Rosentreter et al. (Rosentreter et al., 1998) did not address changes in the ability of growth cones to detect gradients as a function of concentration, as we have done here.

We find that response to a gradient is maximized when receptor binding statistics are pooled spatially over a distance of about one-third of the extent of the growth cone, and that temporal averaging of binding statistics on a timescale of the order of 3 minutes is required to match the sensitivity observed experimentally. The notion of there being an optimal σ_s is one that should apply in any system performing chemotaxis by comparing concentrations across its spatial extent. However, as far as we are aware this is the first time attention has been brought to this phenomenon. A rough calculation gives insight into the optimal value for σ_s as follows:

Consider a one-dimensional sensing device that is a line split up into n equal compartments, each containing about the same number of receptors. Imagine this device is attempting to sense a gradient with steepness m per compartment, i.e. a total concentration change across the device of nm . Assume receptor binding is pooled over k compartments in from each end of the sensing device. The total concentration change between the midpoints of these two pools is now only $(n-k)m$. Conversely, the error in a concentration measurement within each of these pools has now been reduced by a factor of $1/\sqrt{k}$ (Berg and Purcell, 1977). What is the optimal number of compartments over which to average to minimize the steepness of the gradient that can be sensed? Following Berg and Purcell (Berg and Purcell, 1977), threshold detection of the gradient occurs when:

$$\bar{b}_i(t) = \sum_j \bar{b}(t) e^{-(\phi_i - \phi_j)^2 / 2\sigma_s^2}$$

where δb_{bin} is the uncertainty in the concentration measurement for one bin. This can be rewritten as:

$$m = \frac{\sqrt{2\delta b_{\text{bin}}}}{(n-k)\sqrt{k}}$$

To make m as small as possible with respect to k , we differentiate, which gives $k=n/3$.

The intuitive idea is that pooling binding statistics over a spatial region increases the signal-to-noise ratio for the concentration measurement, but decreases the spatial specificity of the measurement. These two competing effects trade off to give the optimal pooling range of one-third of the extent of the sensing device. Although this argument is rough,

it illustrates analytically the plausibility of an optimal spatial scale for the pooling of receptor statistics.

A number of theoretical models have attempted to address the principles involved in growth cone movement (reviewed by Goodhill and Urbach, 2003). For the case of no external ligand gradient, careful quantitative analyses have been performed of axonal trajectories (e.g. Katz et al., 1984; Katz, 1985) and cytoskeletal dynamics including filopodia (Buettner, 1995; Odde and Buettner, 1998), and models have been proposed to capture these general properties (Katz and Lasek, 1985; Li et al., 1994; Hely and Willshaw, 1998). Although models of the behavior of axons in the presence of external gradients exist (Gierer, 1987; Robert and Sweeney, 1997; Hentschel and Van Ooyen, 1999; Goodhill and Urbach, 1999; Goodhill et al., 2004), it has been hard, until now, to compare these quantitatively with experimental data, because suitably controlled measurements have not been available. In particular, the two principal methods used until recently for establishing diffusible gradients *in vitro* (reviewed by Guan and Rao, 2003) are limited in this regard. In the pipette assay (e.g. Zheng et al., 1994; Nishiyama et al., 2003) a defined gradient exists, but the response measured is only whether the growth cone turns over a short period of time, rather than a complete trajectory. In the 3D collagen-gel assay (e.g. Lumsden and Davies, 1983; Charron et al., 2003), the gradient present is not known, and is probably not stable over time (Goodhill, 1997; Goodhill, 1998). The assay introduced by Rosoff et al. (Rosoff et al., 2004) has alleviated this problem, and allows the precise quantitative comparisons with theoretical results of the present paper. The model presented here is related to the model of axonal gradient sensing proposed by Goodhill et al. (Goodhill et al., 2004). In that model, growth cone filopodia were explicitly represented, and guidance was achieved by the preferential generation of filopodia on the up-gradient side (determined as here by noisy receptor-binding measurements) of the growth cone. The growth cone then turned towards the average direction of the filopodia. A comparison of the predictions of that model with the data of Rosoff et al. (Rosoff et al., 2004) reveals an insufficient sensitivity to small gradients (data not shown). In addition to a lack of spatial and temporal averaging, the unavoidably probabilistic nature of filopodia generation in the model contributes a source of noise that acts as a fundamental limitation on sensitivity. The present model is somewhat more abstract, as it does not represent filopodia explicitly.

How might spatial and temporal averaging be implemented biologically? A simple interpretation of spatial pooling of receptor binding statistics is that each receptor-binding event initiates a small release of a downstream signaling molecule, which then spreads out by diffusion so that its effects are combined with release from nearby receptor binding. However, in our model this would require the signaling molecules to diffuse a distance of $3\sigma_s \approx 0.15 \times \pi \times 5 \mu\text{m} \approx 2 \mu\text{m}$ in about $3\sigma_t \approx 3$ minutes, which gives a diffusion constant of the order $10^{-10} \text{ cm}^2/\text{second}$. This seems too small for a freely diffusing molecule in the cytosol, but is plausible for diffusion of molecules in the membrane (Goodhill, 1998; Goodhill and Urbach, 1999). An alternative explanation is therefore that the spatial spread of the effects of receptor binding are mediated through a chain of intermediate signaling components, some of which may be bound to the membrane or cytoskeletal components so that they move and react with each other

relatively slowly. This fits with the picture emerging from experimental data on signal transduction inside growth cones (reviewed by Song and Poo, 2001; Guan and Rao, 2003). A simple interpretation of the duration of temporal averaging is that it corresponds with the decay time of one component of the transduction pathway. However, as for spatial averaging, a more likely possibility is that it is the net effect of several different components that provide inertia to the system.

The present computational results show that adaptation mechanisms are not required to reproduce the most quantitative data currently available on long-term axon guidance by gradients. If growth cones do not adapt, why might they be different from, for instance, bacteria in this regard? One possibility is that they simply do not require adaptation. Current data suggest that single gradients only guide axons for a maximum of about 1 mm in the case of diffusible factors, or about 1 cm in case of substrate bound factors (such as ephrins in the tectum). These distances are consistent with a response over only about 2 to 3 orders of magnitude of absolute concentration (Goodhill and Baier, 1998; Goodhill, 1998; Goodhill and Urbach, 1999), which as we have shown here can be achieved without adaptation. Axonal trajectories tend to be broken up into numerous short segments involving intermediate targets (Tessier-Lavigne and Goodman, 1996). In the highly complex environment of the developing nervous system this may be a more robust strategy than relying on single gradients extended over long distances, and might also provide more combinatorial possibilities for sorting subpopulations of axons (Goodhill, 2003). Although adaptive mechanisms are common in biology, they may have only evolved in cells undergoing chemotaxis when there was a pressing need for guidance over long distances by single gradients.

We thank Ryan McAllister for his contribution to this work. Funding was provided by NIH grant NS046059 as part of the NSF/NIH Collaborative Research in Computational Neuroscience Program, and NIH grant EY014555. G.J.G. also acknowledges support from the Queensland Brain Institute, the School of the Physical Sciences and the Institute for Molecular Biosciences at the University of Queensland.

References

- Baier, H. and Bonhoeffer, F. (1992). Axon guidance by gradients of a target-derived component. *Science* **255**, 472-475.
- Barkai, N. and Leibler, S. (1997). Robustness in simple biochemical networks. *Nature* **387**, 913-917.
- Bennett, D. L. H., Averill, S., Clary, D. O., Priestly, J. V. and McMahon, S. B. (1996). Postnatal changes in the expression of the *trkA* high-affinity NGF receptor in primary sensory neurons. *Eur. J. Neurosci.* **8**, 2204-2208.
- Berg, H. C. and Purcell, E. M. (1977). Physics of chemoreception. *Biophys. J.* **20**, 193-219.
- Bray, D. (1979). Mechanical tension produced by nerve cells in tissue culture. *J. Cell Sci.* **37**, 391-410.
- Bray, D. (2001). *Cell Movements: From Molecules to Motility*. New York, USA: Garland Publishing.
- Bray, D., Levin, M. D. and Morton-Firth, C. J. (1998). Receptor clustering as a cellular mechanism to control sensitivity. *Nature* **393**, 85-88.
- Buettner, H. M. (1995). Computer simulation of nerve growth cone lopotial dynamics for visualization and analysis. *Cell Motil. Cytoskeleton* **32**, 187-204.
- Charron, F., Stein, E., Jeong, J., McMahon, A. P. and Tessier-Lavigne, M. (2003). The morphogen sonic hedgehog is an axonal chemoattractant that collaborates with netrin-1 in midline axon guidance. *Cell* **113**, 11-23.

- Dickson, B. J.** (2002). Molecular mechanisms of axon guidance. *Science* **298**, 1959-1964.
- Gallo, G., Lefcort, F. B. and Letourneau, P. C.** (1997). The trkA receptor mediates growth cone turning toward a localized source of nerve growth factor. *J. Neurosci.* **17**, 5445-5454.
- Gierer, A.** (1987). Directional cues for growing axons forming the retinotectal projection. *Development* **101**, 479-489.
- Goodhill, G. J.** (1997). Diffusion in axon guidance. *Eur. J. Neurosci.* **9**, 1414-1421.
- Goodhill, G. J.** (1998). Mathematical guidance for axons. *Trends Neurosci.* **21**, 226-231.
- Goodhill, G. J.** (2003). A theoretical model of axon guidance by the robo code. *Neural Comput.* **15**, 549-564.
- Goodhill, G. J. and Baier, H.** (1998). Axon guidance: stretching gradients to the limit. *Neural Comput.* **10**, 521-527.
- Goodhill, G. J. and Urbach, J. S.** (1999). Theoretical analysis of gradient detection by growth cones. *J. Neurobiol.* **41**, 230-241.
- Goodhill, G. J. and Urbach, J. S.** (2003). Axon guidance and gradient detection by growth cones. In *Modeling Neural Development* (ed. A. Van Ooyen), pp. 95-109. Cambridge, Massachusetts: MIT Press.
- Goodhill, G. J., Gu, M. and Urbach, J. S.** (2004). Predicting axonal response to molecular gradients with a computational model of lopotial dynamics. *Neural Comput.* **16**, 2221-2243.
- Gordon-Weeks, P. R.** (2000). *Neuronal Growth Cones: The Molecular Approach to Their Behaviour*. Cambridge, UK: Cambridge University Press.
- Guan, K. L. and Rao, Y.** (2003). Signalling mechanisms mediating neuronal responses to guidance cues. *Nat. Rev. Neurosci.* **4**, 941-956.
- Hely, T. A. and Willshaw, D. J.** (1998). Short term interactions between microtubules and actin lamellae underlie long term behaviour in neuronal growth cones. *Proc. R. Soc. London B Biol. Sci.* **265**, 1801-1807.
- Hentschel, H. G. E. and Van Ooyen, A.** (1999). Models of axon guidance and bundling during development. *Proc. R. Soc. London B Biol. Sci.* **266**, 2231-2238.
- Huber, A. B., Kolodkin, A. L., Ginty, D. D. and Cloutier, J. F.** (2003). Signaling at the growth cone: ligand-receptor complexes and the control of axon growth and guidance. *Annu. Rev. Neurosci.* **26**, 509-563.
- Iglesias, P. and Levchenko, A.** (2002). Modeling the cell's guidance system. *Sci. STKE* **148**, RE12.
- Katz, M. J.** (1985). How straight do axons grow? *J. Neurosci.* **5**, 589-595.
- Katz, M. J. and Lasek, R. J.** (1985). Early axon patterns of the spinal cord: experiments with a computer. *Dev. Biol.* **109**, 140-149.
- Katz, M. J., George, E. B. and Gilbert, L. J.** (1984). Axonal elongation as a stochastic walk. *Cell Motil.* **4**, 351-370.
- Koshland, D. E., Goldbeter, A. and Stock, J. B.** (1982). Amplification and adaptation in regulatory and sensory systems. *Science* **217**, 220-225.
- Li, G.-H., Qin, C.-D. and Li, M.-H.** (1994). On the mechanisms of growth cone locomotion: modeling and computer simulation. *J. Theoret. Biol.* **169**, 355-362.
- Lumsden, A. G. S. and Davies, A. M.** (1983). Earliest sensory nerve fibres are guided to peripheral targets by attractants other than nerve growth factor. *Nature* **306**, 786-788.
- Macnab, R. M. and Koshland, D. E.** (1972). The gradient-sensing mechanism in bacterial chemotaxis. *Proc. Natl. Acad. Sci. USA* **69**, 2509-2512.
- Meakin, S. O. and Shooter, E. M.** (1992). The nerve growth family of receptors. *Trends Neurosci.* **15**, 323-331.
- Meinhardt, H.** (1999). Orientation of chemotactic cells and growth cones: models and mechanisms. *J. Cell Sci.* **112**, 2867-2874.
- Ming, G.-l., Wong, S. T., Henley, J., Yuan, X. B., Song, H. J., Spitzer, N. C. and Poo, M.-m.** (2002). Adaptation in the chemotactic guidance of nerve growth cones. *Nature* **417**, 411-418.
- Molliver, D. C. and Snider, W. D.** (1997). Nerve growth factor receptor TrkA is down-regulated during postnatal development by a subset of dorsal root ganglion neurons. *J. Comp. Neurol.* **381**, 428-438.
- Mu, X., Silos-Santiago, I., Carroll, S. L. and Snider, W. D.** (1993). Neurotrophin receptor genes are expressed in distinct patterns in developing dorsal root ganglia. *J. Neurosci.* **9**, 4029-4041.
- Nishiyama, M., Hoshino, A., Tsai, L., Henley, J. R., Goshima, Y., Tessier-Lavigne, M., Poo, M.-m. and Hong, K.** (2003). Cyclic AMP/GMP-dependent modulation of Ca²⁺ channels sets the polarity of nerve growth cone turning. *Nature* **424**, 990-995.
- Odde, D. J. and Buetner, H. M.** (1998). Autocorrelation function and power spectrum of two-state random processes used in neurite guidance. *Biophys. J.* **75**, 1189-1196.
- Parent, C. A. and Devreotes, P. N.** (1999). A cell's sense of direction. *Science* **284**, 765-770.
- Phillips, H. S. and Armanini, M. P.** (1996). Expression of the trk family of neurotrophin receptors in developing and adult dorsal root ganglion neurons. *Philos. Trans. R. Soc. London Ser. B* **351**, 413-416.
- Piper, M., Salih, S., Weini, C., Holt, C. E. and Harris, W. A.** (2005). Endocytosis-dependent desensitization and protein synthesis-dependent resensitization in retinal growth cone adaptation. *Nat. Neurosci.* **8**, 179-186.
- Robert, M. E. and Sweeney, J. D.** (1997). Computer model: investigating role of lopotia-based steering in experimental neurite galvanotropism. *J. Theor. Biol.* **188**, 277-288.
- Rosentreter, S. M., Davenport, R. W., Loschinger, J., Huf, J., Jung, J. and Bonhoeffer, F.** (1998). Response of retinal ganglion cell axons to striped linear gradients of repellent guidance molecules. *J. Neurobiol.* **37**, 541-562.
- Rosoff, W. J., Urbach, J. S., Esrick, M., McAllister, R. G., Richards, L. J. and Goodhill, G. J.** (2004). A novel chemotaxis assay reveals the extreme sensitivity of axons to molecular gradients. *Nat. Neurosci.* **7**, 678-682.
- Song, H. and Poo, M.-m.** (1999). Signal transduction underlying growth cone guidance by diffusible factors. *Curr. Opin. Neurobiol.* **9**, 955-969.
- Song, H. and Poo, M.-m.** (2001). The cell biology of neuronal navigation. *Nat. Cell Biol.* **3**, E81-E88.
- Tessier-Lavigne, M. and Placzek, M.** (1991). Target attraction – are developing axons guided by chemotropism? *Trends Neurosci.* **14**, 303-310.
- Tessier-Lavigne, M. and Goodman, C. S.** (1996). The molecular biology of axon guidance. *Science* **274**, 1123-1133.
- Zheng, J. Q., Felder, M., Conner, J. A. and Poo, M.-m.** (1994). Turning of growth cones induced by neurotransmitters. *Nature* **368**, 140-144.
- Zheng, J. Q., Wan, J.-j. and Poo, M.-m.** (1996). Essential role of lopotia in chemotropic turning of nerve growth cone induced by a glutamate gradient. *J. Neurosci.* **16**, 1140-1149.